LETTER

Novel Hydrophilic Bis(1,2,3-triazolyl)fluorenyl Probe for In vitro Zinc Ion Sensing

Dao M. Nguyen,[†] Xuhua Wang,[†] Hyo-Yang Ahn,[†] Luis Rodriguez,[†] Mikhailo. V. Bondar,[‡] and Kevin D. Belfield*[,†,§]

Department of Chemistry and CREOL, The College of Optics and Photonics, University of Central Florida, 4000 Central Florida Parkway, Orlando, Florida 32816, United States, and Institute of Physics, Prospect Nauki, 46, Kiev-28 03094, Ukraine

ABSTRACT A hydrophilic bis(1,2,3-triazolyl)fluorene derivative was synthesized as a multi-photon-absorbing, zinc-ion-sensing fluorescent probe. The fluorescence response was approximately five-fold greater in presence of Zn^{2+}, resulting in a large binding constant (1×10^9) for a 1:2 ligand to zinc complex. A four-fold increase in the two-photon absorption cross section was achieved upon binding Zn^{2+}. In vitro two-photon fluorescence microscopy imaging revealed a significant fluorescence increase upon introduction of Zn^{2+} into HeLa cells and reversible Zn^{2+} binding, demonstrating the potential of this probe for zinc ion sensing.

KEYWORDS: 1,2,3-triazolyl-fluorene • two-photon microscopy bioimaging • fluorescent probe • zinc ion sensing • metal sensing • binding constant

Zinc is the second most abundant transition metal ion in vivo and plays a significant role in the metabolic regulation, ion channels and receptors, neuronal transmission, and certain metalloenzymes (1, 2). In neurophysiology, zinc ion is thought to participate in the formation of β-amyloid in Alzheimer's disease (3). Zinc ion release also causes hypoglycemia-induced neuronal death (4). The zinc ion is relatively inert with a closed shell of $3d^{10}$ electronic configuration, hence fluorescence methods are advantageous for detection of Zn^{2+} (5, 6).

Designing new fluorescent probes for Zn^{2+} sensing in vitro and in vivo in biological environments should involve selectivity for Zn^{2+} over other relevant metal ions. The probe should have high affinity, as well as bind rapidly and reversibly. Zinc ion sensing utilizing fluorescein (7), porphyrin (8), benzoxazole (9), and other derivatives (10) have been reported. Since the advent of two-photon absorption (2PA) and techniques that rely on 2PA, a number of advantages have been identified for 2PA, e.g., molecules can be excited at a long wavelength, usually in the near infrared (NIR) region, deeper penetration and less scattering, and reduced photodamage and photobleaching (11). Recently, our laboratory developed 2PA fluorescent probes for targeting cellular proteins (12, 13) and other biological applications. The fluorene-based construct is employed for its generally high fluorescence quantum yield, reasonably large 2PA cross section, and high photostability (14−19).

The metal sensing probe reported herein is constructed of an acceptor-π-electron bridge-donor (A−π−D) fluorene-based chromophore system, consisting of a 1.2,3-triazole-based recognition moiety for an integrated fluoroionophore (5). The bis(1,2,3-triazolyl)fluorene-based probe was synthesized by "click" chemistry (20, 21), and it exhibited signifcantly enhanced fluorescence emission upon binding Zn^{2+} ions over other biologically relevant heavy metals. The linear and nonlinear photophysical properties of the new probe **1** were investigated in common solvents. The metal to ligand stoichiometry ratio and the binding constant were determined, as was the reversibility of metal complexation. In vitro cell imaging revealed a fluorescence enhancement upon introduction of Zn^{2+} ions, and was reversible, as described below.

Bis(1,2,3-triazolyl)fluorene **1** was synthesized from fluorene derivative **A** (Scheme 1), involving a Sonogashira coupling of **A** with 2-(4-ethynylphenyl)benzothiazole **B** to obtain **C**, followed by reduction using hydrazine on Pd/C in a mixture of EtOH and THF at 70 °C to yield **D**. Arylamine **D** underwent N-alkylation with propargyl bromide affording bis-alkyne **E**. Finally, a "click" reaction of **E** and 2-azidoethylacetate, using copper(I) catalyst at room temperature, afforded bis(1,2,3-triazolyl)fluorene **1** in 70% yield. 2-Azidoethylacetate was prepared by a new method and its NMR spectra were consistent with the literature (22). The HRMS of **1** confirmed a molecular ion at 980.4249, which is consistent for the formula $C_{54}H_{60}O_8N_8S$.

Bis(1,2,3-triazolyl)fluorene **1** exhibited high thermal stability as the thermogravimetric analysis (TGA) of **1** showed it decomposed above 300 °C (see Figure S3 in the Supporting Information).

The linear photophysical properties of **1** in ethanol, acetonitrile, aqueous acetonitrile, THF, and cell medium (RPMI) are summarized in Table 1. The UV−vis absorption

* Corresponding author. E-mail: belfield@mail.ucf.edu. Fax: (407) 823-2252.
Received for review August 11, 2010 and accepted October 22, 2010
[†] Department of Chemistry, University of Central Florida.
[‡] Institute of Physics.
[§] CREOL, The College of Optics and Photonics, University of Central Florida.
DOI: 10.1021/am100719v

Published on Web 10/28/2010

Scheme 1. Synthesis of Bis(1,2,3-triazolyl)fluorene 1

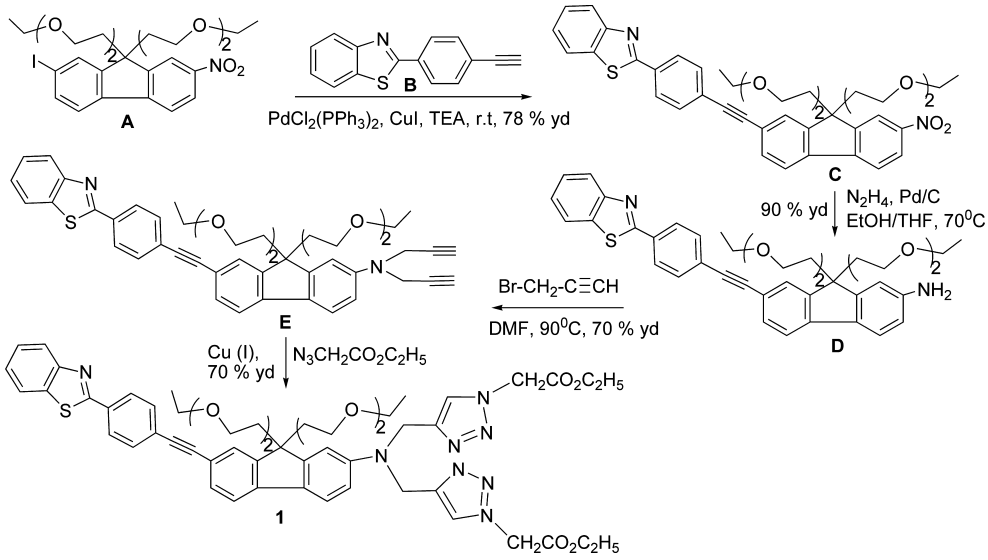

Table 1. Linear Photophysical Properties of 1 and Select Metal Complexes in Solution

solvent	metal ion	ϕ_{Fl}	τ (ns)	$\varepsilon \times 10^{-4}$ ($M^{-1}cm^{-1}$)	λ_{ab} (nm)	λ_{em} (nm)	$\Delta\lambda$
EtOH	**1**	0.1[a]	0.3	7	383	613	230
	1 + Zn^{2+}	0.3	1.6		366	513	149
	1 + Hg^{2+}	0.1			362	550	180
	1 + Cd^{2+}	0.2			372	568	196
	1 + Pb^{2+}	0.1			381	595	214
ACN	**1**	0.1		6	385	643	258
	1 + Zn^{2+}	0.3			368	568	200
ACN:H_2O (95:5)	**1**	0.02			384	663	279
ACN: H_2O (95:5)	**1** + Zn^{2+}	0.04			369	627	258
THF		0.9		7.2	390	568	178
RPMI	**1**	0.37			395	555	160
	1 + Zn^{2+}	0.44			388	514	126

[a] Photodecompostition quantum yield (23) at 405 nm, $\phi_D = 2 \times 10^{-6}$.

and fluorescence emission of **1** with metal ions in common organic solvents were quite similar. The fluorescence emission of **1** displayed a large Stokes shift with increasing solvent polarity (see Figure S4 in the Supporting Information).

Several relevant metal ions were evaluated with the new probe **1** by UV–vis absorption and fluorescence emission spectroscopy. The fluorescence response factor (F/F_0) was measured by comparison of the maximum integrated area of the corrected emission spectrum of the metal complex (F) with the probe **1** before addition of metal ion (F_0). The UV–vis absorption of **1** with selected heavy metal ions (Zn^{2+}, Hg^{2+}, Cd^{2+}, Pb^{2+}) showed a hypsochromic shift from 2 to 20 nm. The fluorescence emissions of metal ions Li^+, Mg^{2+}, Ca^{2+}, Ba^{2+}, Fe^{2+}, Co^{2+}, Cu^+, Hg^+, La^{3+}, and Au^{3+} were relatively unchanged, whereas Cu^{2+}, Fe^{3+}, and Pd^{2+} quenched the fluorescence. However, Hg^{2+}, Cd^{2+}, Ag^+, Pb^{2+}, and Zn^{2+} enhanced the fluorescence (Figure 1). The UV–vis absorption and fluorescence emission of **1** with Zn^{2+} in ethanol were blue-shifted that could be due to the increase in energy gap between the HOMO–LUMO as a function of Zn^{2+} concentration with isosbestic points with a single equilibrium complexation (see Figure S5 in the Supporting Information). Moreover, an approximately five-fold fluorescence increase upon binding to Zn^{2+} (Figure 2) resulted in a large binding constant of 1×10^9 M^{-2} for a 1:2 ligand to metal stoichiometry ratio, determined by the linear fitting (see Figure S6 in the Supporting Information) (24). The fluorescence quantum yield and lifetime dramatically increased for Zn^{2+} complex-

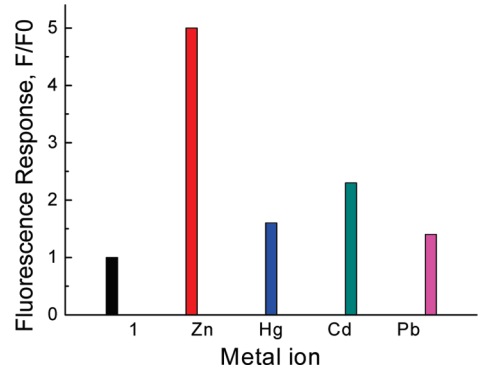

FIGURE 1. Fluorescence response of 1 at 2×10^{-6} M in ethanol towards selected metal ions in concentrations ranging from 1×10^{-6} to 1×10^{-4} M.

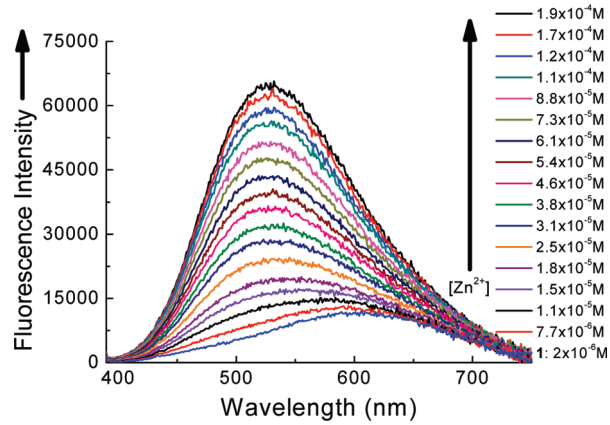

FIGURE 2. Fluorescence emission spectra of 1 at 2×10^{-6} M in ethanol excited at 383 nm as a function of Zn^{2+} concentration.

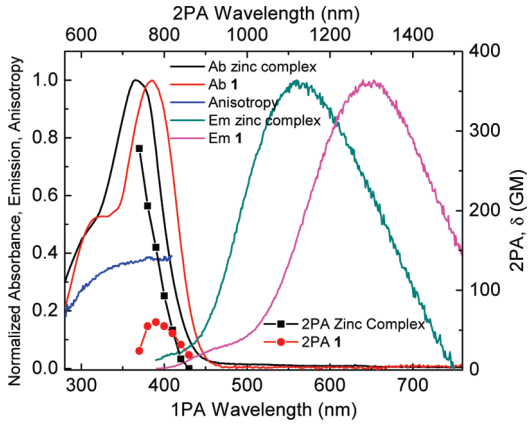

FIGURE 3. UV−vis absorption, fluorescence emission, anisotropy, and 2PA of 1 and its zinc complex at 1×10^{-4} M in ACN.

ation with **1** in comparison to the free probe **1** (Table 1). The behavior of **1** in cell medium (pH 7.4) and in acetic acid buffer (25) (pH 5) was unchanged. However, at lower pH (<4), the emission spectrum showed an additional absorption at 450 nm due to the protonated form, and at a higher pH (>9) the compound precipitated.

The complex of **1** with metal ions formed rapidly upon agitation and was stable for several days. Moreover, complexation with **1** was reversible as demonstrated by displacement with EDTA (ethylenediamine tetracarboxylic acid), liberating probe **1** from its zinc complex (see Figure S7 in the Supporting Information).

Figure 3 illustrates the two-photon absorption (2PA) cross-sections of **1** and its zinc complex in ACN. A significant increase in the 2PA cross section in region $\lambda = 740-760$ nm was observed for the complex relative to free **1**. The 2PA process is a third-order nonlinear optical property with a strong dependence on the intramolecular charge transfer (ICT) process (26). The observed increase in δ_{2PA} of its zinc complex suggests that metal binding does not occur primarily via the amino functionality, rather it is suggestive of binding to the 1,2,3-triazolyl carboxylate moieties, since binding the the electron-donating moiety would be expected to decrease ILCT and the δ_{2PA} (10a, 27, 28). The nature of Zn ion binding to this class of molecule and its dependence on 2PA is complex and a subject of future investigation.

The 2PA cross sections of the zinc complex of **1** at 740−760 nm were ca. 100−280 GM, suitable for applications in two-photon fluorescence microscopy (2PFM) zinc ion sensing and imaging.

The cytotoxicity of probe **1** was evaluated by the Alamar Blue cytotoxicity assay to assess its suitability for in vitro imaging (29). Relatively low cytotoxicity of **1** in HeLa cells was demonstrated with optimal concentrations for imaging at 5−15 μM (see Figure S8 in the Supporting Information).

In vitro Zn^{2+} sensing and 2PFM imaging was investigated for probe **1** in live HeLa cells (Figure 4); cells were maintained on a stage incubator and images were acquired before and after a zinc containing medium was introduced into cells. Next, *N*,*N*,*N*′,*N*′-tetrakis(2-pyridylmethyl)ethylenediamine (TPEN) was introduced as a chelator (30) to displace

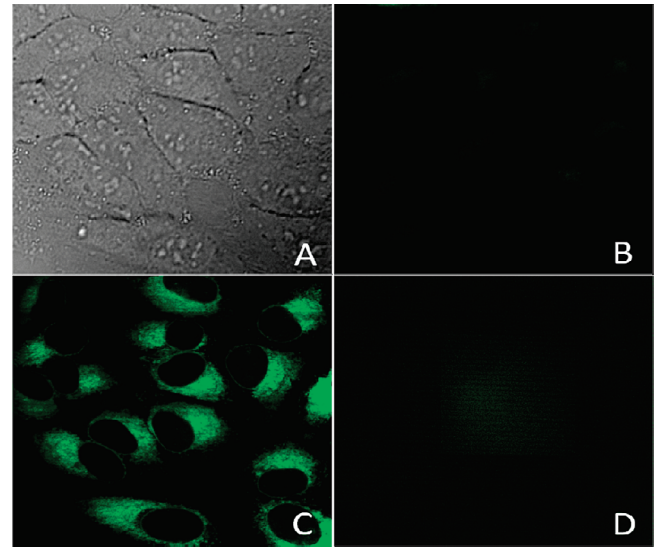

FIGURE 4. (A) DIC image of HeLa cells incubated with 15 μM of probe 1 for 2 h. (B) 2PFM image at $\lambda_{ex} = 740$ nm and power = 50 mW. (C) 2PFM image after 15 min treatment with zinc sulfate (50 μM). (D) 2PFM image after further incubation with 50 μM TPEN for 15 min.

Zn^{2+} in the zinc complex of **1**, resulting in a decrease in fluorescence (Figure 4B−D) in vitro.

The new probe **1** exhibited both good two-photon absorptivity and fluorescence enhancement upon Zn^{2+} binding, had low cytotoxicity, had high Zn^{2+} binding constants, and, importantly, was soluble in aqueous media. Bis(1,2,3-triazolyl)fluorene **1** proved useful for in vitro zinc ion sensing by 2PFM, suggesting future potential for in vivo Zn^{2+} sensing and imaging, a subject of future investigation.

Acknowledgment. This work was supported by the National Institutes of Health (1 R15 EB008858-01), the National Science Foundation (CHE-0832622 and CHE-0840431), the U.S. Civilian Research and Development Foundation (UKB2-2923-KV-07), and the Ministry of Education and Science of Ukraine (Grant M/49-2008).

Supporting Information Available: Synthesis and NMR spectra of **1**, TGA analysis, photophysical characterization, additional UV−vis absorption and emission spectra, binding constant determination of **1** with Zn^{2+} ion, reversibility, viability assay of probe **1** in HeLa cells, and experimental cell incubation and imaging (PDF). This material is available free of charge via the Internet at http://pubs.acs.org.

REFERENCES AND NOTES

(1) Bush, A. I. *Curr. Opin. Chem. Biol.* **2000**, *4*, 184–191.
(2) Maret, W. *Biometals* **2001**, *14*, 187–190.
(3) Bush, A. I. *Trends. Neurosci.* **2003**, *26*, 207–214.
(4) Suh, S. W.; Garnier, P.; Aoyama, K.; Chen, Y.; Swanson, R. A. *Neurobiol. Disease* **2004**, *16*, 538–545.
(5) Valeur, B.; Leray, I. *Coord. Chem. Rev.* **2000**, *205*, 3–40.
(6) Barrios, A. M. *ACS Chem. Biol.* **2006**, *1*, 67–68.
(7) (a) Walkup, G. K.; Burdette, S. C.; Lippard, S. J.; Tsien, R. Y. *J. Am. Chem. Soc.* **2000**, *122*, 5644–5645. (b) Hirano, T.; Kikuchi, K.; Urano, Y.; Higuchi, T.; Nagano, T. *J. Am. Chem. Soc.* **2000**, *122*, 12399–12400. (c) Chang, C. J.; Nolan, E. M.; Jaworski, J.; Okamoto, K.-I.; Hayashi, Y.; Sheng, M.; Lippard, S. J. *Inorg. Chem.* **2004**, *43*, 6774–6779.
(8) (a) Nolan, E. M.; Lippard, S. J. *Acc. Chem. Res.* **2009**, *42*, 193–203. (b) Zhang, X.-A.; Lovejoy, K. S.; Jasanoff, A.; Lippard, S. J. *Proc. Natl. Acad. Sci. U.S.A.* **2007**, *104*, 10780–10785.

(9) Taki, M.; Wolford, J. L.; O'Halloran, T. V. *J. Am. Chem. Soc.* **2004**, *126*, 712–713.
(10) (a) Sumalekshmy, S.; Henary, M. M.; Siegel, N.; Lawson, P. V.; Wu, Y.; Schmidt, K.; Bredas, J.-L.; Perry, J. W.; Fahrni, C. J. *J. Am. Chem. Soc.* **2007**, *129*, 11888–11889. (b) Kim, H. M.; Seo, M. S.; An, M. J.; Hong, J. H.; Tian, Y. S.; Choi, J. H.; Kwon, O.; Lee, K. J.; Cho, B. R. *Angew. Chem. Int. Ed.* **2008**, *47*, 5167–5170. (c) Kim, H. M.; Cho, B. R. *Acc. Chem. Res.* **2009**, *42*, 863–872. (d) Chen, X.-Y.; Shi, J.; Li, Y.-M.; Wang, F.-L.; Wu, X.; Guo, Q.-X.; Liu, L. *Org. Lett.* **2009**, *11*, 4426–4429.
(11) Denk, W.; Strickler, J. H.; Webb, W. W. *Science* **1990**, *248*, 73–76.
(12) Morales, A. R.; Schafer-Hales, K. J.; Marcus, A. I.; Belfield, K. D. *Bioconjugate Chem* **2008**, *19*, 2555–2567.
(13) Morales, A. R.; Yanez, C. O.; Schafer-Hales, K. J.; Marcus, A. I.; Belfield, K. D. *Bioconjugate Chem.* **2009**, *20*, 1992–2000.
(14) Belfield, K. D.; Hagan, D. J.; Stryland, E. W.; Shafer, K. J.; Negres, R. A. *Org. Lett.* **1999**, *1*, 1575–1578.
(15) Schafer, K. J.; Belfield, K. D.; Yao, S.; Frederiksen, P. K.; Hales, J. M.; Kolattukudy, P. E. *J. Biomed. Opt* **2005**, *10*, 051402-1–051402-8.
(16) Corredor, C. C.; Belfield, K. D.; Bondar, M. V.; Przhonska, O. V.; Yao, S. *J. Photochem. Photobiol., A* **2006**, *184*, 105–112.
(17) Belfield, K. D.; Bondar, M. V.; Przhonska, O. V.; Schafer, K. J. *J. Photochem. Photobiol., A* **2004**, *162*, 489–496.
(18) Belfield, K. D.; Bondar, M. V.; Przhonska, O. V.; Schafer, K. J. *J. Photochem. Photobiol., A* **2004**, *162*, 569–574.
(19) Belfield, K. D.; Bondar, M. V.; Pzhonska, O. V.; Schafer, K. J. *J. Photochem. Photobiol. Sci.* **2004**, *3*, 138–141.
(20) (a) Huisgen, R. *Proc. Chem. Soc.* **1961**, *10*, 357–369. (b) Huisgen, R. *Angew. Chem., Int. Ed.* **1963**, *2*, 565–598. (c) Huisgen, R. *Angew. Chem., Int. Ed.* **1963**, *2*, 633–645.
(21) Kolb, H. C.; Finn, M. G.; Sharpless, K. B. *Angew. Chem., Int. Ed* **2001**, *40*, 2004–2021.
(22) Shi, F.; Waldo, J. P.; Chen, Y.; Larock, R. C. *Org. Lett.* **2008**, *10*, 2409–2412.
(23) Belfield, K. D.; Bondar, M. V.; Liu, Y.; Przhonska, O. V. *J. Phys. Org. Chem.* **2003**, *16*, 69–78.
(24) Videva, V.; Chauvin, A.-S.; Varbanov, S.; Baux, C.; Scopelliti, R.; Mitewa, M.; Bunzli, J.-C. G. *Eur. J. Inorg. Chem* **2004**, *25*, 2173–2179.
(25) Ruzin, S. E. *Plant Microtechnique and Microscopy*; Oxford University Press: New York, 1999; p 224.
(26) Valeur, B.; Leray, I. *Coord. Chem. Rev.* **2000**, *205*, 3–40.
(27) Das, S.; Nag, A.; Sadhu, K. K.; Goswami, D.; Bharadwaj, P. K. *J. Organomet.Chem.* **2007**, *692*, 4969–4977.
(28) Ahn, H. C.; Yang, S. K.; Kim, H. M.; Li, S.; Jean, S.-J.; Cho, B.-R. *Chem. Phys. Lett.* **2005**, *410*, 312–315.
(29) Shahan, T. A.; Siegel, P. P.; Sorenson, W. G.; Kuschner, W. G.; Lewis, D. M. *J. Immunol. Methods* **1994**, *175*, 181–187.
(30) Blindauer, C. A.; Razi, M. T.; Parsons, S.; Sadler, P. J. *Polyhedron* **2006**, *25*, 513–520.

AM100719V